Thermochimica Acta, 207 (1992) 65–78
Elsevier Science Publishers B.V., Amsterdam

High-temperature DTA of transuranium materials with application to the Np–Zr phase diagram

John K. Gibson and Richard G. Haire

Transuranium Research Laboratory, Chemistry Division, Oak Ridge National Laboratory, Oak Ridge, TN 37831-6375 (USA)

(Received 3 February 1992)

Abstract

A high-temperature thermal analysis system has been developed for the study of highly radioactive and scarce transuranium materials. Modifications to a commercial instrument (Perkin-Elmer DTA-1700) for installation and operation in an argon-atmosphere, radioactive-containment glove box are described. The argon atmosphere permitted the handling of air-sensitive and moisture-sensitive samples (e.g. metals), and initial studies have been made on the phase relations in selected actinide alloy systems. Procedures for preparing and studying alloys are described, and preliminary results obtained from our exploratory DTA studies of the Np–Zr alloy system are presented and discussed.

INTRODUCTION

Experimental data for the thermal properties of a variety of actinide materials are required for the development of new technological applications and for a better understanding of the fundamental behavior of the actinides. Of special interest in the latter regard is the role of the 5f electrons in the bonding and electronic properties of the actinide elements. Metallic transuranium (TRU) fuel materials have been proposed for applications in advanced reactor concepts, and investigation of the high-temperature phase relationships of the TRU elements and some selected alloys is of interest. Owing to their scarcity and/or radioactivity, it is desirable to carry out investigations on TRU materials using minimum-sized samples. Because differential thermal analysis (DTA) is inherently well suited to the investigation of relatively small samples, it offers a particularly appropriate approach for studying the high-temperature thermal properties of TRU elements and compounds.

Correspondence to: John K. Gibson, Chemistry Division, Bldg. 5505, MS-6375, P.O. Box 2008, Oak Ridge National Laboratory, Oak Ridge, TN 37831-6375, USA.

The actinide metals display various levels of air- and moisture-sensitivity, and it is therefore necessary to use inert atmospheres in handling and studying them. To provide the containment and the inert atmosphere required for handling samples of TRU metals and alloys, we have developed a facility which incorporates a commercial high-temperature DTA/DSC instrument into an inert atmosphere glove box which has special provisions for the containment and handling of these radioactive materials (TRU DTA facility).

One potentially limiting aspect of the use of neptunium- or plutonium-based metallic fuels is the anomalously low melting points of these two elements ($T_{\mathrm{fus}}[\mathrm{Np}] = 639°\mathrm{C}$, $T_{\mathrm{fus}}[\mathrm{Pu}] = 640°\mathrm{C}$ [1]). It has been suggested [2] that the β-form (body-centered cubic (bcc)) of zirconium would be completely miscible with the high-temperature (γ, also bcc) form of neptunium, which, based upon ideal solution behavior, would dramatically elevate the melting point of a neptunium-containing phase relative to pure neptunium. Although data for the U–Zr [3] and Pu–Zr [4] phase diagrams would tend to support this prediction, experimental studies on the phase relations in the Np–Zr system have not been reported.

In the initial phase of our studies of actinide alloys using the TRU DTA facility, we have undertaken to establish the essential nature (e.g. miscibility or immiscibility; pseudo-ideal or non-ideal solution behavior) of the Np–Zr binary alloy system. In addition to describing this DTA facility and operating procedures, preliminary results obtained from our exploratory DTA studies of the Np–Zr system are presented and discussed.

EXPERIMENTAL

Inert atmosphere containment system

A high-temperature (1500°C maximum) DTA/DSC instrument (Perkin-Elmer model DTA-1700) was modified as described below and installed into an inert atmosphere glove box (Vacuum/Atmospheres Co. (V/A) model HE) which had been modified to allow for handling of the highly radioactive TRU elements. In the case of relatively small, laboratory-scale (e.g. multi-milligram) samples of Np, Pu or Am, the potential for significant personnel exposure due to the penetrating radiation field (e.g. neutron and γ-radiation) does not pose a problem. Rather, the primary consideration is the potential for internal personnel contamination in the event of the inadvertent release of material to the laboratory environment. It is thus possible to handle such samples of the TRU elements in sealed glove boxes without additional shielding, provided that adequate consideration is given to minimizing the possibility for breach of containment. To allow for the handling of air-sensitive materials, it is necessary to utilize a glove box capable of maintaining inert atmospheres for such containment.

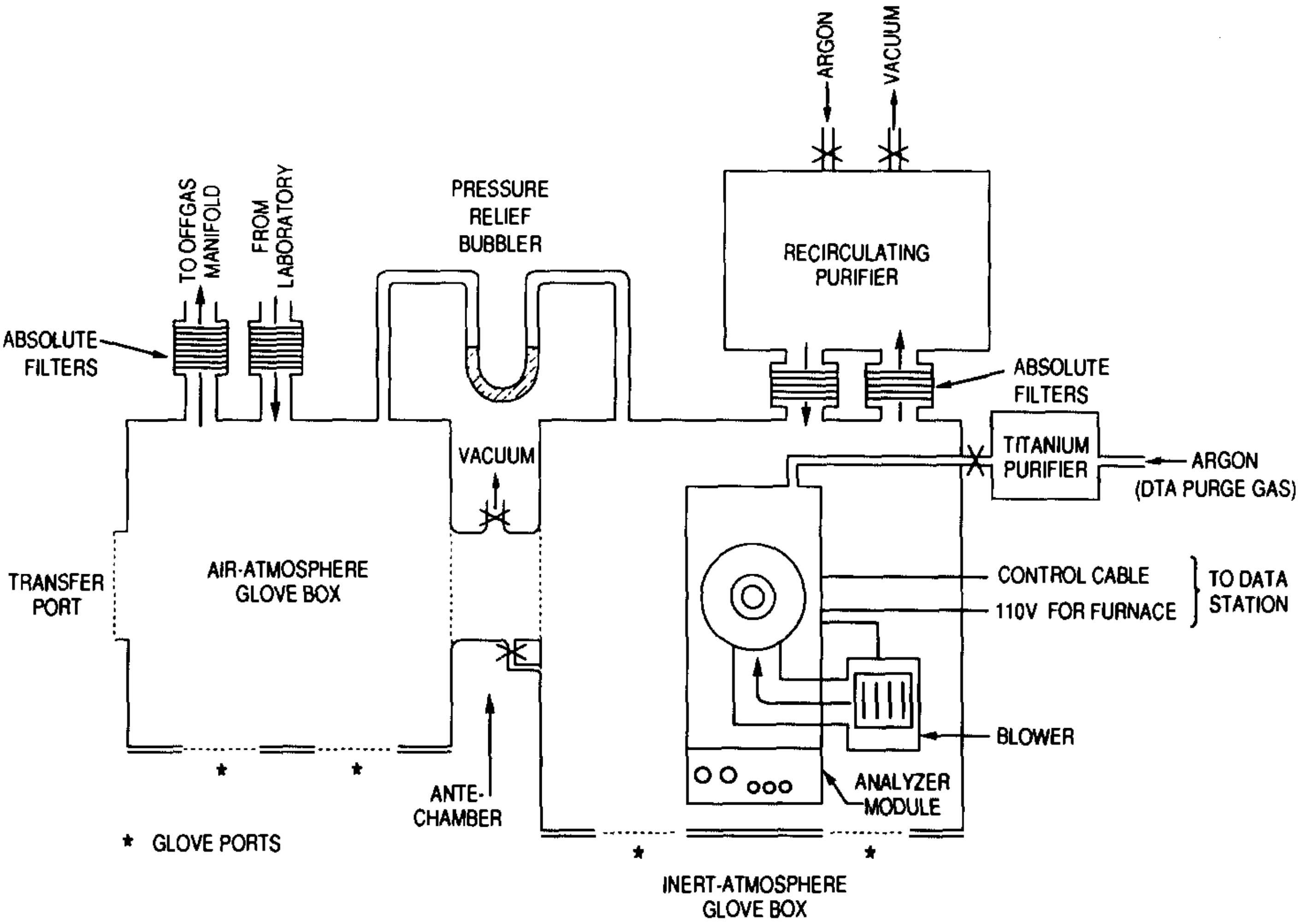

Fig. 1. Schematic of the transuranium DTA facility. The primary components of the DTA apparatus and glove box system are shown (not to scale); details are discussed in the text.

The primary components of the TRU DTA facility are shown schematically in Fig. 1. Figure 2 shows a photograph of the glove box assembly; included is a view of the DTA analyzer inside the inert (right-hand-side) glove box. The two aluminum glove boxes (each 45 inches wide × 30 inches deep) are interconnected by an evacuable (to 1 Pa) ante-chamber. The standard windows and skylights were replaced with 1/2 inch thick polycarbonate (Lexan) for extra strength. Four glove ports were installed into each window to allow access to the entire box volumes; the heavy (0.8 mm thick) butyl rubber gloves are relatively impervious to the inflow of contaminating gases and provide good breach-resistance. The air-atmosphere, alpha-containment box on the left (Figs. 1 and 2) serves primarily as an interface between the inert-atmosphere box and the laboratory, although it is also used for other non-air-sensitive operations. All transfers between the laboratory and the glove boxes are via a bag-in/bag-out port in the air-box which retains isolation of the box interior from the laboratory. Transfers between the air-box and the argon-box are through the evacuable ante-chamber, which preserves the purity of the argon atmosphere. The air-box is maintained under dynamic flow at a negative pressure of about 10 mm water column relative to the laboratory by connection through absolute filters to an exhaust system.

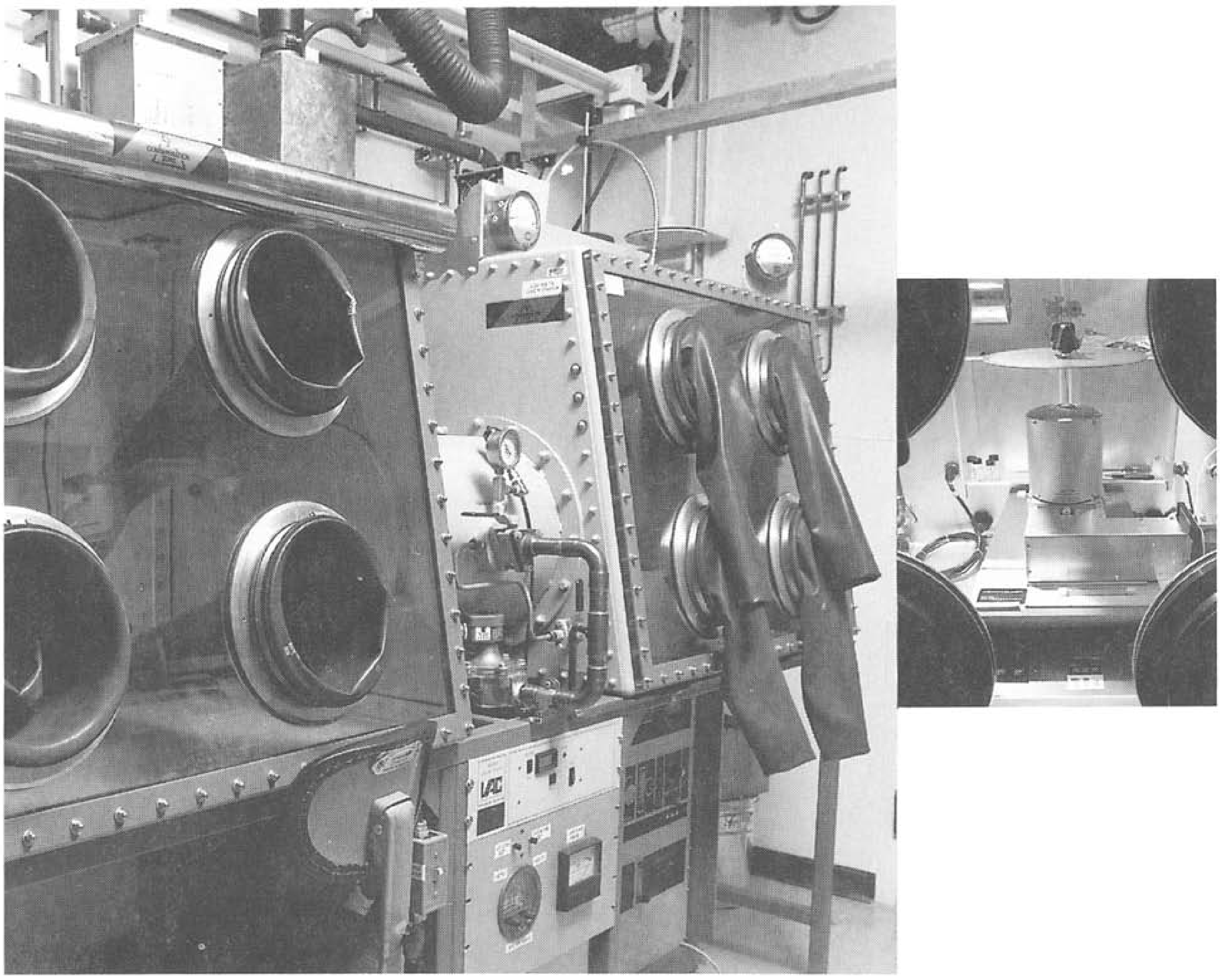

Fig. 2. Photograph of the transuranium DTA facility. The components are as indicated in Fig. 1. On the right is a view of the analyzer inside the inert-atmosphere glove box.

Design and operation of the inert atmosphere box for the DTA was more critical because it is inherently a closed-loop, continuous purification system. One particular concern was the heating of the atmosphere by the DTA furnace and the resulting pressure increase in the box. Argon was selected as the inert atmosphere since excessive heat loss through a more conductive gas, such as helium, would have interfered with operation of the DTA furnace, and a nitrogen atmosphere would offer the potential for formation of metal nitrides. Water and oxygen atmosphere impurities are continuously removed from the box atmosphere by a recirculating (19 l s^{-1}) purification system (V/A model MO-40-2H); the purifier is maintained free of radioactive contamination using in-line absolute (HEPA) filters between it and the glove box. Moisture is generally the most reactive contaminant in the box atmosphere and its level is routinely maintained below 1 ppm as monitored with an Al_2O_3 sensing probe (V/A model AM-2031); although not measured directly in this system oxygen levels in similar systems are maintained below 10 ppm. The level of nitrogen contamination is not quantitatively measured, but the preservation of metallic samples over extended periods suggests that it is maintained at an acceptably low level, presumably by routine replenishment of the box atmosphere with virgin argon (e.g. through pressure control during routine operations and when the box atmosphere is used to refill the evacuated ante-chamber).

Three control systems are provided to prevent over- or under-pressurization of the inert-box. Routine pressure control (typically between −25 mm and +25 mm water column during operations and between −8 mm and +8 mm water column while unattended) is via the manual or automatic (photohelic) control of solenoid valves which supply argon or vacuum through the purifier. Automatic control is used to maintain the pressure within the preset range while the box is unattended, and during operation of the DTA furnace, when heating of the box atmosphere can result in significant increases in pressure. The second (backup) pressure control Photohelic system closes solenoid valves in all lines which connect the box to pressure or vacuum sources in the event that wider setpoint limits (typically −50 mm to +50 mm water column during operations and −25 mm to +25 mm water column while unattended) are exceeded. The final, fail-safe pressure control system is an oil-filled bubbler (free of valves) connected to the adjacent air-atmosphere box, which adjusts the pressure in the inert-box if the pressure differential exceeds ±65 mm water column. This last pressure is well below a gradient which would result in the failure of any component necessary for maintaining containment.

Modifications to the DTA instrumentation

Installation of the DTA instrument in the argon-atmosphere glove box required modifications to the instrument's standard configuration. The control and power cables between the DTA-1700 Analyzer and the System 7/4 Controller were adapted to hermetically-sealed bulkhead feedthroughs in the wall of the box. The System 7/4 and 3700 Data Station were therefore located about 3 m away from the analyzer, with no apparent deterioration in the performance of the instrument. The argon purge gas for the sample region of the analyzer is passed through a purifier (titanium metal at 900°C; R.D. Mathis Co. model GP-100) and then enters through another box feedthrough. A 25 cm diam. disk of thin stainless steel directly above the DTA furnace serves as a heat shield and minimizes radiative heating of the top of the glove box. The temperature of the entire box atmosphere increases typically by ≈ 10°C when the furnace was heated to 1400°C; the automatic primary pressure control system maintains the box pressure.

It was not practical to introduce large volumes of gas into the inert glove box for cooling the furnace/sample assembly as recommended for the DTA-1700. Instead, a closed-loop circulating system using the argon-box atmosphere provides the desired cooling. A 60 $\mathrm{l\ s^{-1}}$ blower, activated when the cooling gas solenoid circuit in the DTA-1700 is energized by the controller, forces the box atmosphere through a duct to the base of the furnace. This system was found to provide more than adequate cooling; for example, when such cooling was initiated at the end of a heating run, the sample temperature fell from 1400 to 1000°C in 4 min, to 500°C in 10 min and to 100°C in 20 min. Such cooling rates were generally excessive for controlled cooling runs and the gas flow had to be reduced or eliminated to obtain useful DTA cooling curves.

DTA procedures

Materials and containment

The neptunium used in the experiments was isotopically pure ^{237}Np, which undergoes alpha-decay with a half-life of 2.1×10^6 y. Neptunium metal was prepared in batches of 200–500 mg by reduction of NpF_4 with calcium metal. The procedures used for preparation of research samples of the actinide metals have been described in detail elsewhere [5]. An analysis of each metal preparation was not practical, but spark source mass spectrographic analysis of representative samples indicated that the cationic (metallic) impurity levels were maintained below 200 wt. ppm. With these relatively small metal samples, it is not feasible to analyze for anionic impurities such as oxygen, nitrogen and hydrogen. To minimize contamination of the Np metal by gaseous impurities, the metal was prepared using a vacuum of better than 1×10^{-5} Pa; all subsequent handling of the materials was carried out in inert-atmosphere (helium or argon) glove boxes. Each neptunium sample studied by DTA had a mass of 30–100 mg, consisting of 1–4 pieces of bulk metal. The zirconium metal used here was 1 mm diam. wire (Johnson Matthey) with a vendor-specified purity of 99.8%.

The DTA studies of the Np–Zr alloy system were carried out using the pure metals and an in situ alloying approach. Weighed portions of the two metals were introduced into the DTA sample container and heated to above the fusion point of neptunium to permit alloying. An equilibrium alloy sample is most effectively prepared by heating above the fusion points of all of the constituents. However, this was not possible in our studies of the Np–Zr alloy system because the DTA-1700 is not capable of achieving the melting temperature of zirconium (1852°C). Therefore, it was necessary to employ procedures to ensure that the final alloys were representative of equilibrium products. For example, DTA thermograms of the samples were obtained until the locations and magnitudes of the peaks remained constant, which was indicative of equilibration.

The use of an in situ alloying technique has two primary advantages. Efficient use is made of the TRU metal since the entire alloy specimen is studied without losses due to external preparation and transfer. A second and more generally relevant advantage of in situ alloying is that it provides an initial baseline thermogram for the pure component element(s) for comparison with results subsequently obtained for the alloy in the identical experimental arrangement. With the Np–Zr system, for example, the initial heating run provided a thermogram for the transitions due to neptunium prior to fusion, for comparison with the DTA results obtained after alloying with zirconium. Potentially, it is possible to study a series of alloy compositions by successive additions (titrations) of one component to the other(s), obtaining thermograms after each addition. The utility of this titration approach with many metal samples, and particularly with actinide metals, may be limited by reaction of the sample with the container and/or by losses resulting from wetting, creeping or vaporization of one or more components.

Given the reactivity of neptunium (and other actinides) and zirconium at elevated temperatures, sample containment must be given careful consideration. The use of platinum crucibles with either Zr or Np at high temperature would result in the formation of platinum intermetallic compounds (e.g. $ZrPt_3$ [6]). Our experimentation with lanthanide metals (as surrogates for the actinides) embedded in high-purity Al_2O_3 powder resulted in unacceptable oxidation of the metals, especially upon their fusion. The vendor-supplied 60 mm^3 Al_2O_3 cups, without any diluent powder, were found to be suitable for the molten neptunium alloys at temperatures up to 1420°C; only a slight degree of oxidation of the sample was evident at its interface with the container wall. Considering this (minor) interaction between the sample and the cup, a new Al_2O_3 cup was used for each sample. Tantalum cells were also found to be suitable for containing molten lanthanide/actinide metals [7]. For some of the experiments, small Ta cells with an internal volume of about 20 mm^3 served as liners inside the 60 mm^3 alumina sample cups. Although tantalum has been used to study actinide metals and alloys with minimal sample contamination [8], zirconium is known to alloy with tantalum [6]; zirconium and tantalum may thus interact at high temperatures, especially where one is in a liquid form (e.g. as a component of a molten Np–Zr alloy). Separate experiments using alumina and tantalum to contain the metal samples were carried out for the Np–Zr system in order to establish that the DTA results were independent of the container material used. Both types of containers easily accommodated neptunium metal samples of up to 100 mg. Loose-fitting tantalum lids on the alumina cups or the tantalum cells minimized the exposure of the reactive metal samples to any impurities in the flowing argon purge. Although not a significant concern for low vapor pressure metals such as Np and Zr, the lids can also serve to minimize sample vaporization. In all of the DTA experiments described here, the reference was a tantalum cell containing alumina powder.

Calibration

The temperature calibration of the DTA instrument was accomplished by measuring the onset temperatures for the solid–solid transformations of SiO_2 (573°C) and $BaCO_3$ (808 and 968°C), both ICTA standard reference materials supplied by the National Institute of Standards and Technology. The measured temperatures were generally within a few degrees of the known equilibrium transition temperatures. Because the in situ alloying technique effectively provides an internal standard of the pure metal(s) at the start of each experiment, rigorous calibration of the absolute temperatures was not critical for the Np–Zr studies. Further, given the magnitude of the expected effects upon the transitions (especially the liquidus), establishing the essential nature of phase relations in the Np–Zr alloy system was not expected to require refined transition temperatures.

Heating and cooling curves were generally obtained with the instrument operating in the differential scanning calorimeter (DSC) mode so that transition enthalpies could be derived from the integrated peak areas. An approximate instrument sensitivity factor (ISF) for these enthalpy determinations was obtained by measuring the solid–solid transition enthalpies of the SiO_2 and $BaCO_3$ standards [9] and the fusion enthalpies of the pure lanthanide metals Ce°, Sm° and Pr° [10] (the lanthanide metals were at least of 99.9% cationic purity, according to specifications by the vendor). Based upon the scatter in the calibrant measurements, the average ISF was considered accurate to ±20%. No systematic variation of the ISF to within 20% was observed over the measured temperature range and a temperature-averaged ISF was used. As with the transition temperatures, relative comparison of the measured enthalpies for the pure constituents with those obtained after they had alloyed provided the most effective method for assigning the alloy transitions. In fact, the reproducibility/accuracy of the measured Np–Zr alloy enthalpies, in particular, proved to be rather limited, and the enthalpy comparisons were largely qualitative. All of the oxide and metal standards were run in the same type of tantalum cell as that used for the alloy studies. Although a few cooling thermograms were obtained, all of the calibrations and most of the alloy measurements were made using a heating rate of 10°C min^{-1}.

RESULTS FROM THE Np–Zr ALLOY STUDIES

Prior to investigating the Np–Zr alloy system by DTA, each component was individually studied to provide reference thermograms. As little as 30 mg (0.11 mmol) of pure Np gave sharply defined DTA peaks for the two solid–solid transformations and the melting transition. The average measured onset temperatures and transition enthalpies for neptunium were α(orthorhombic) $\rightarrow$ β(tetragonal), 282°C (6.6 kJ mol^{-1}); $\beta \rightarrow \gamma$(bcc), 578°C (3.9 kJ mol^{-1}); and $\gamma \rightarrow$ liq., 640°C (4.2 kJ mol^{-1}). As will be discussed in detail in a report describing our recent DTA investigations of phase relations in the Np–Am alloy system [8], these values are in good agreement with those reported in the literature. Cooling curves obtained with pure neptunium showed that these elemental transitions were reversible, as expected, with only slight depressions in their onset temperatures.

The high (1852°C) melting point of zirconium precluded its observation with the DTA-1700. However, zirconium metal does undergo an allotropic transformation from its room temperature hexagonal-close-packed (hcp) crystalline modification (α form) to the high-temperature bcc structure (β form) at $T_{\alpha \to \beta} = 863(5)$°C, with an associated enthalpy of $\Delta_{\alpha \to \beta}H = 3.89(8)$ kJ mol^{-1} [6]. In contrast to the sharp peaks observed for the lower-temperature neptunium transitions, it was found that the zirconium allotropic transformation resulted in a relatively broad and shallow, almost indistinct, DTA peak (about 70° wide using a heating rate of 10°C min^{-1}). Thus, although a peak for this transition could be observed with a 27 mg (0.30 mmol) sample of zirconium, values for the onset temperature and enthalpy could only be approximated as being 840(10)°C and 3(1) kJ mol^{-1}, respectively. Pure zirconium was studied only to 1100°C, well below the zirconium melting point, and visual inspection of the material at the conclusion of the measurements suggested that an interaction with the tantalum crucible had not occurred. The zirconium allotropic transformation ($\alpha \to \beta$) could not be definitively detected for quantities of zirconium as small as were used for most of the alloy studies. Therefore, given these limitations it was possible only to monitor the neptunium transitions in the Np–Zr alloy studies.

In conjunction with our DTA investigations of selected actinide–actinide and actinide–lanthanide binary alloy systems carried out in parallel with the work described here [8], proof-of-principle experiments were carried out using selected binary lanthanide alloy samples as surrogates (e.g. Ce–Sm). These supporting studies confirmed the efficacy of the experimental method used here, and particularly that the in situ alloying approach provides an effective means for preparing equilibrium alloy samples in the DTA apparatus.

Based upon known phase diagrams of the binary alloy systems U–Zr [3] and Pu–Zr [4], it would be predicted that the Np–Zr phase diagram should be characterized by complete miscibility of the bcc γ-Np and the bcc β-Zr phases with a resulting alloy liquidus curve reflecting nearly ideal solution behavior (i.e. a nearly linear variation in liquidus temperature with composition between 640°C for pure Np and 1852°C for pure Zr). Beahm [2] has used the Kaufman method and a regular solution model to calculate a Np–Zr phase diagram that is in accord with this prediction. The technological significance of such ideal solution behavior would be that the melting point of a Np–Zr alloy would then be significantly elevated relative to pure Np, and it was this aspect of the phase diagram which was being investigated in the present studies. The existence and nature of other (lower temperature) phases, for example, was of secondary interest.

Given the predicted dramatic increase in the liquidus temperature with even small additions of zirconium, it was anticipated that such behavior could be readily verified by studying only a few alloy compositions. The addition of 20 at.% Zr to Np, for example, would be expected to elevate the liquidus temperature by about 240°C, from 640°C for pure Np to 880°C for a $Np_{0.8}$–$Zr_{0.2}$ alloy; such an effect would be easily detected by DTA. As discussed below, the observed behavior was not as predicted and could not be considered indicative of a near-ideal Np–Zr alloy.

Two sets of DTA experiments on the Np–Zr system were carried out. For the first, 67 mg of Np° was placed with 7 mg of Zr° in a tantalum cell to provide a net composition of 22 at.% Zr–Np. The thermogram from the first heating (to 900°C at 10°C min^{-1}) is shown as the top curve in Fig. 3; the three peaks due to neptunium metal transitions are identified. The only significant change in subsequent thermograms obtained after the sample had been heated to 1200°C was the splitting of the 575°C peak of Np ($\Delta H = 1.10$ J) into a doublet, with $T_{onset} \approx 553$°C (ΔH[doublet] ≈ 1.0 J). Visual inspection of the sample at the end of this series of heatings suggested that a substantial amount of the zirconium remained as a separate phase (largely undissolved).

An additional 19 mg of zirconium was added to this composite to provide a new net composition of 50 at.% Zr–Np. The thermogram obtained after heating this new composition to 1400°C is shown in the bottom of Fig. 3; the essential features of this curve remained largely unchanged after repeated cycling to temperatures up to 1400°C and no additional peaks were evident. Upon cooling this sample at 5°C min^{-1}, the 638°C peak appeared with nearly the same onset temperature (640°C) and enthalpy (2.95 J); the minor, lower-temperature (≈ 511°C) peak was indistinct upon cooling but may have been obscured by the relatively poor baseline observed during cooling. It should be noted that the small exotherm/endotherm spike, evident at 588°C in the bottom curve of Fig. 3, is an experimental artifact which persisted in blank thermograms obtained after the Zr–Np sample had been removed; this effect was attributed to undesirable deposits in the sample and/or reference regions of the system and was subsequently eliminated by replacement of the thermocouples and other components.

To investigate the effect of the cell's material on the experimental results, a second series of experiments was performed using an alumina cup to study a virgin Np–Zr sample. Combining 12 mg of zirconium with 33 mg of neptunium provided a net composition of 48 at.% Zr–Np, close to the final net composition of the alloy discussed above. Again, the three transitions for pure neptunium metal were observed on the first heating curve. After heating of the samples to 1400°C, the subsequent thermograms

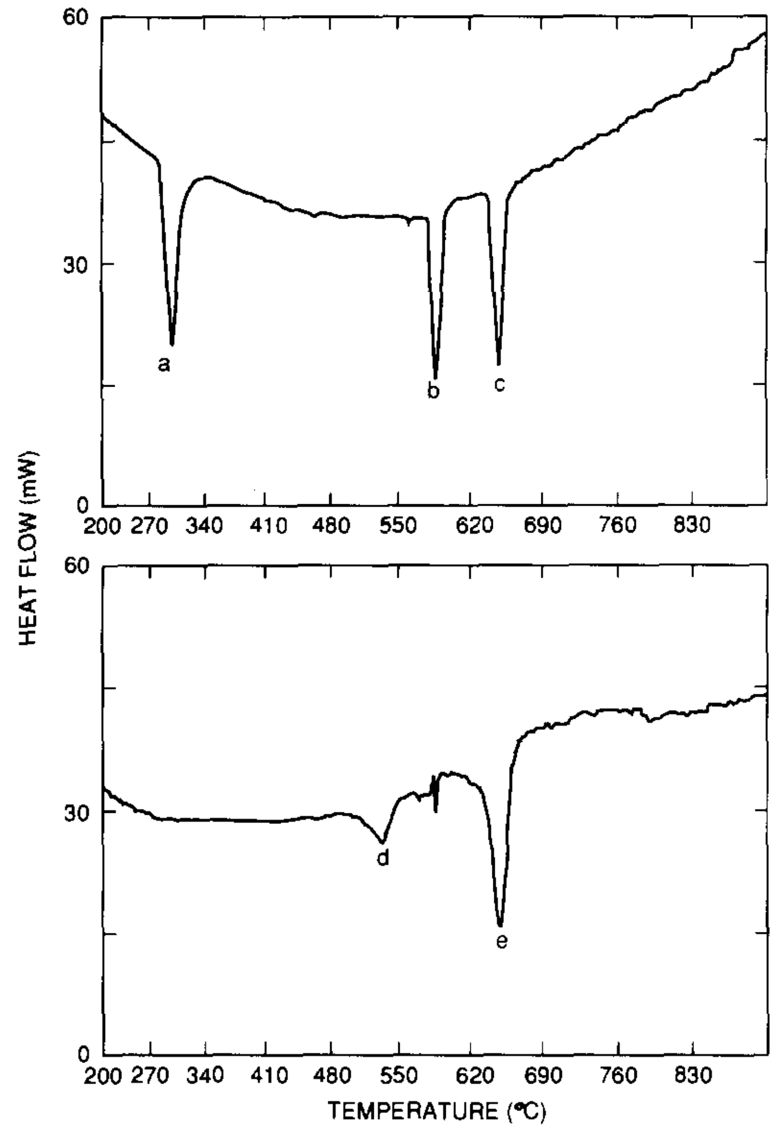

Fig. 3. DSC curves for the system Np + Zr. Heating rate, +10°C min^{-1}. Tantalum sample container. The downward peaks indicate endothermic transitions. Top: Initial heating of 66.9 mg Np$^{\circ}$ + 7.1 mg Zr$^{\circ}$ (aggregate composition, 22 at.% Zr). The three peaks are assigned to unalloyed Np$^{\circ}$ transitions with measured onset temperatures and enthalpies: (a) $\alpha \rightarrow \beta$, $T_{tr} = 281°C$, $\Delta_{tr}H = 1.81$ J (6.4$_2$ kJ per mol Np); (b) $\beta \rightarrow \gamma$, $T_{tr} = 575°C$, $\Delta_{tr}H = 1.10$ J (3.8$_8$ kJ per mol Np); (c) $\gamma \rightarrow$ liq., $T_{fus} = 636°C$, $\Delta_{fus}H = 1.15$ J (4.0$_6$ kJ per mol Np). Bottom: Heating of 66.9 mg Np$^{\circ}$ + 25.7 mg Zr$^{\circ}$ (aggregate composition, 50 at.% Zr) after heating to 1400°C. The onset temperatures and enthalpies are (d) 511°C, 0.57 J; (e) 638°C, 2.26 J.

exhibited reproducibly a large peak with an onset temperature of 640°C ($\Delta H = 1.7$ J) and a much smaller peak ($\Delta H \approx 0.2$ J) at $\approx 540°C$. It is significant that the main features of these curves were in agreement with those for the $\approx 50\%$ composition that had been studied in the tantalum cell (i.e. Fig. 3, bottom). It is also noted that heating of this second (48 at.%) Zr–Np sample to intermediate temperatures (e.g. to 800°C), prior to homogenization at higher temperatures, resulted in DTA curves similar to those for the more dilute (22 at.%) Zr–Np alloy (in Ta cell). Our interpretation of this observation is that partial alloying of the 48% net composition at lower temperature produced an alloy with a lower Zr content. The evident approach to the equilibrium alloy composition from the pure components is illustrative of the progress of in situ alloying, and illustrates the method of obtaining a constancy of DTA results to confirm such equilibration.

As a final step, an additional 27 mg of zirconium was added to the 48 at.% Zr–Np sample in the Al_2O_3 cup to provide a new net composition of 75 at.% Zr–Np. After homogenizing the sample by heating to 1400°C, the resulting alloy system gave heating curves characterized by only a single peak at ≈ 540°C ($\Delta H \approx 0.6$ J).

CONCLUSIONS

For all of the Np–Zr compositions studied, significant changes in the alloy thermograms were evident when compared with the pure element thermograms. For example, with the 75 at.% and the two ≈ 50 at.% Zr–Np samples, the low-temperature peak due to the $\alpha \rightarrow \beta$ transition of neptunium was entirely absent. Such alterations in the observed thermograms indicated that some zirconium was dissolved. In accord with this, it was apparent from the physical appearance of the samples after the experiments that, although dissolution of the zirconium metal was incomplete, some substantial interaction between the two component metals had occurred.

It is apparent from the results for the ≈ 20 at.% and ≈ 50 at.% Zr–Np samples that the expected dramatic elevation in the melting point of neptunium by the addition of zirconium did not occur; this further suggests that the bcc phases of Zr and Np are not completely miscible. In fact, the onset temperature of the peak for the transition assigned to the liquidus of the neptunium-rich alloy phase in these Np–Zr samples remained essentially unchanged relative to the congruent melting point of pure neptunium. These initial results suggest that the addition of zirconium may not prove an effective means for elevating the melting point of metallic neptunium fuels, and that the form of the Np–Zr phase diagram may be fundamentally different (i.e. immiscible, non-ideal) from those of the U–Zr and Pu–Zr (miscible, ideal) systems.

Concurrent with the disappearance of the Np $\alpha \rightarrow \beta$ (and perhaps also $\beta \rightarrow \gamma$) transition(s) (281 and 575°C in pure Np) in both of the ≈ 50 at.% Zr–Np alloys was a substantial increase in the enthalpy associated with the high-temperature (fusion) transition. It might be speculated that the bcc form of neptunium was stabilized by the addition (perhaps of even small amounts) of zirconium, and that the enthalpy associated with one or both of the solid–solid transitions of pure neptunium is subsumed into the melting transition in the alloy. Based upon our observations, it would appear that the transition which appeared at ≈ 540°C in each of the Np–Zr alloys studied is associated with some Zr-rich phase, either a terminal solid solution or an intermediate phase; in accord with this interpretation, this was the only transition observed for the 75 at.% Zr–Np alloy.

It should be re-emphasized that the exploratory results reported here for the Np–Zr system should be considered preliminary and are presented primarily to illustrate the application of this new DTA facility. Although these surprising results do offer some insight concerning the essential character of the Np–Zr phase diagram (i.e. immiscible, non-ideal), clarification of the details of the phase relations in this system will require additional investigation. Especially useful in this regard would be DTA studies of Np–Zr alloy samples prepared by other techniques, such as arc-melting; such supplemental studies would most importantly serve to confirm that equilibrium alloy specimens were indeed generated by the in situ preparative technique used here. X-ray powder diffraction structural determinations and other supporting analytical characterizations of Np–Zr alloy samples would further aid in the detailed delineation of the phase diagram. Given the unexpectedly unique (immiscible) nature of the Np–Zr phase diagram (compared with the U–Zr and Pu–Zr diagrams) suggested by the results reported here, such confirmatory and expanded studies are especially important.

ACKNOWLEDGMENTS

Research sponsored by the Division of Chemical Sciences, Office of Basic Energy Sciences, U.S. Department of Energy, under Contract DE-AC05-84OR21400 with Martin Marietta Energy Systems, Inc.

The authors gratefully acknowledge the interests and efforts of Drs. E.C. Beahm and S. Raman of Oak Ridge National Laboratory; and Dr. T. Ogawa and Mr. T. Mukaiyama of the Japan Atomic Energy Research Institute (JAERI). Their contributions led to the development of this program for the experimental investigation of actinide phase diagrams. The differential thermal analyzer used in this work was supplied by the JAERI.

REFERENCES

1 M.V. Nevitt and M.B. Brodsky, in J.J. Katz, G.T. Seaborg and L.R. Morss (Eds.), The Chemistry of the Actinide Elements, 2nd edn., Vol. 2, Chapman and Hall, New York, 1986, p. 1388.
2 E.C. Beahm, Oak Ridge National Laboratory, personal communication, 1989.
3 R.I. Sheldon and D.E. Peterson, Bull. Alloy Phase Diagrams, 10 (1989) 165.
4 J.A.C. Marples, J. Less-Common Met., 2 (1960) 331.
5 R.G. Haire, J. Less-Common Met., 21 (1986) 379.
6 C.B. Alcock, K.T. Jacob, S. Zador, O. Kubaschewski-von Goldbeck, H. Nowotny, K. Seifert and O. Kubaschewski, in O. Kubaschewski (Ed.), Zirconium: Physico-Chemical Properties of its Compounds and Alloys, Special Issue No. 6, International Atomic Energy Agency, Vienna, 1976.
7 D.H. Dennison, M.J. Tschetter and K.A. Gschneidner, Jr., J. Less-Common Met., 11 (1966) 423.

8 J.K. Gibson and R.G. Haire, J. Nucl. Mater., in press.
9 O. Kubaschewski and C.B. Alcock, Metallurgical Thermochemistry, 5th edn., Pergamon, New York, 1979, p. 326.
10 K.A. Gschneidner, Jr., in D.R. Lide (Ed.), CRC Handbook of Chemistry and Physics, 71st edn., CRC Press, Boston, 1990, p. 4-119.